scientific reports

Check for updates

OPEN

Oxidative stress biomarkers for assessing the synergistic toxicity of emamectin benzoate and cyantraniliprole on liver function

Yaxuan Zhang[1,5], Yuxin Xiang[1,3,5], Zhiyong Cao[1,3], Kaijie Dai[1,3], Shuyan Gui[3], Yuying Liu[1,3], Ziqi Liu[1,3], Yanhong Shi[2,3], Haiqun Cao[1,3] & Jinjing Xiao[1,3,4]✉

Multiple pesticide residues in agricultural products and environments, especially those with synergistic toxicity, pose a potential risk to human health. We observed a remarkable increase in serum biochemical parameters related to rat liver function when rat liver was exposed to the binary mixture of emamectin benzoate and cyantraniliprole. The present study aimed to investigate the toxicity interactions and underlying mechanisms of the binary mixture by using an L-02 cell model and metabolomics analysis. Cytotoxicity tests have shown that binary mixtures of emamectin benzoate and cyantraniliprole produced either additive or synergistic toxic effect on the cell viability of the human hepatic epithelial cell line L-02. The interaction within the binary mixtures resulted in the production of excessive reactive oxygen species (ROS) and malondialdehyde, as well as overexpression of antioxidant enzyme activities. The synergism was driven by aggravated production of ROS, leading to an imbalance in mitochondrial oxidation and energy metabolism, suggesting the possible use of ROS as an effective toxicity endpoint. Based on the benchmark dose calculated to determine the combined toxicity threshold, the model-averaged estimates of the benchmark dose lower confidence limits (4.74–9.58 mmol/L) of the binary mixtures at concentration ratios of 3:15, 3:45, 4:15, and 4:45 were 20% more toxic than their individual active ingredients. These findings have important implications for risk assessments of pesticide residue in food and highlight the need to consider concentration ratios and oxidative stress endpoints in such assessments.

Keywords Pesticide residues, Synergism, Oxidative stress, Benchmark dose, L-02 cells

Concerns about the risks of co-exposure to multiple pesticide residues have gained global attention. Pesticides are indispensable in agricultural production, and their formulations frequently contain several active ingredients aimed at managing resistance and broadening the spectrum of pest control. Consequently, multiple pesticide residues are commonly detected in food[1,2]. Evidence suggests that interactions among these active ingredients within a mixture can lead to altered toxicity profiles, including additive or synergistic/antagonistic adverse effects[3]. This suggests that mixtures could induce toxic effects even when present at concentrations below their individual no-observed-adverse-effect levels (NOAELs). Understanding mixture exposure therefore warrants specific investigation to guide the reasonable application of pesticides.

In the case of multiple pesticide residues, understanding their combined action and toxicity endpoints is crucial for establishing the threshold for their combined toxicity[4]. One critical factor to consider is how changes in the relative proportions of the individual active ingredients within the mixture can influence the interactions and, consequently, the toxicity. For instance, Huang et al. reported a shift in the interaction profile of a binary mixture of aldicarb and methomyl from synergism to additive action, and then to antagonism, as the concentration of aldicarb increased[5]. Another challenge in assessing combined toxicity is the selection of appropriate toxic endpoints to better represent adverse biological effects. Studies have indicated that traditional

[1]Joint Research Center for Food Nutrition and Health of IHM, School of Plant Protection, Anhui Agricultural University, Hefei, China. [2]College of Resource & Environment, Anhui Agricultural University, Hefei 230036, Anhui, China. [3]Key Laboratory of Agri-Products Quality and Biosafety (Anhui Agricultural University), Ministry of Education, Hefei 230036, Anhui, China. [4]School of Resource & Environment, Anhui Agricultural University, 130 West Changjiang Road, Hefei 230036, Anhui, People's Republic of China. [5]These authors contributed equally: Yaxuan Zhang and Yuxin Xiang. ✉email: xiaojj187012@163.com

toxicity endpoints based on tissue[6] and individual levels, such as histopathology[7], behavior[8], and survival[9], can indicate chemical-induced adverse effects at the population level, but lack sufficient sensitivity and specificity for predictive risk assessment. These considerations underscore the need to develop sensitive toxicity endpoints and elucidate combined effects across varying concentration-effect ratios to predict combined toxicity.

Among the various organs susceptible to pesticide toxicity, the liver, owing to its extensive metabolic activity, is the primary target[10]. Epidemiological studies have demonstrated that pesticide exposure can trigger oxidative stress[11], metabolic disruptions[10], and mitochondrial damage[12] within the liver. Furthermore, such exposure elevates the risk of hepatocellular carcinoma hepatocellular carcinoma[13]. Consequently, liver toxicity has been proposed as a potential indicator for assessing public health risks associated with pesticide exposure. In this regard, in vitro human cell-based models are critical, serving as essential tools for hazard characterization and viable alternatives to traditional animal testing strategies[14]. The human hepatic epithelial cell line L-02, initially derived from a human normal liver cell line, retains numerous characteristics of hepatocytes, rendering them a commonly used choice for toxicity evaluation[15]. Particularly, the combination of in vitro cell models with metabolomics can identify potential biomarkers for monitoring combined toxicity of pesticide mixtures at the cellular level[16].

Emamectin benzoate, a macrocyclic lactone insecticide derived from the avermectin class[17], and cyantraniliprole, a second-generation diamide insecticide[18], are widely recognized for their efficacy against a diverse range of pests. Their exceptional effectiveness against *Spodoptera frugiperda* (J.E. Smith) has drawn significant attention to the development of a binary mixture formulation[19]. However, studies have revealed that exposure to either emamectin benzoate or cyantraniliprole may pose hepatotoxic risks, leading to liver injury[20]. Previous studies have also indicated the presence of emamectin benzoate or cyantraniliprole residual mixtures in agricultural products[11]. Therefore, this study employed the L-02 cells model combined with a metabolomics approach to assess the combined toxicity and the potential underlying mechanisms of the binary mixtures of emamectin benzoate and cyantraniliprole on the liver. The results provide theoretical insights into the complex toxic interactions and the development of pesticide limits.

Materials and methods

Chemicals and reagents

Analytical standards of emamectin benzoate (99.9% purity) and cyantraniliprole (99.8% purity) were acquired from *ANPEL* Laboratory Technologies Inc. (Shanghai, China). Standard stock solutions of the pesticides were prepared in dimethyl sulfoxide (DMSO) and diluted to a series of concentrations with cell culture medium. Biochemical kits used in the study were obtained from Beyotime Biotechnology (Shanghai, China). Other chemicals and solvents were purchased from Innochem (Beijing) Technology Co., Ltd, China.

Animals and treatment

All methods are conducted and reported in accordance with the ARRIVE guidelines. The animal care and experimental protocols were approved by the Institutional Animal Care Committee of Anhui Agricultural University (AHAUXMSQ 2024094) in accordance with its guidelines.

A total of 32 mice were used for the toxicity study. The mice (C57BL/6J, 6 weeks old) were purchased from Hangzhou Ziyuan Experimental Animal Technology Co. Ltd. (Zhejiang, China) and acclimated for 1 week under standard animal house conditions (light/dark cycle of 12/12-h, temperature of 22 ± 2 °C, and relative humidity of 50 ± 5%). Food and water were available ad libitum. For the exposure studies, the mice were randomly assigned to control ($n = 8$) and experimental groups ($n = 8$). During the exposure, the mice were treated with 0.2 mL of 0.9% sterile saline containing emamectin benzoate (5 mg/kg·bw), cyantraniliprole (25 mg/kg·bw), or their binary mixture (5 + 25 mg/kg·bw) by oral gavage. Control mice received equal amounts of sterile saline by gavage. After a 10-day pesticide exposure, carbon dioxide inhalation method was gradually used to induce anesthesia and euthanasia in mice. Then, their blood samples were collected to measure serum biochemical parameters related to liver function. Briefly, serum samples were separated by centrifugation at 1000×*g* for 20 min and stored at − 80 °C until analysis. The serum levels of alanine aminotransferase (ALT), aspartate aminotransferase (AST), total bilirubin (TBIL), direct bilirubin (DBIL), albumin (ALB), alkaline phosphatase (ALP), γ-glutamyl transpeptidase (γ-GT), and total bile acid (TBA) were determined using commercially available kits (Servicebio, Wuhan, China), using an automatic biochemical analyzer (ADVIA2400, Siemens, USA).

Cell culture

L-02 cells (NTCC [@] CVCL 6926™) were procured from Warner Bio-LOGY (Wuhan, China) and cultured under the following conditions: 37 °C, 5% CO_2, and 90% relative humidity. Cell maintenance was performed using Roswell Park Memorial Institute 1640 (RPMI-1640) medium supplemented with 10% (*v*/*v*) fetal bovine serum and 1% penicillin–streptomycin solution. The culture medium was replaced every 48 h until the cells reached 80% confluence. Subsequently, the cells were trypsinized using a 0.25% trypsin-ethylenediaminetetraacetic acid solution and resuspended in RPMI-1640 medium for subsequent experiments.

Cell viability assay

The combined toxicity on emamectin benzoate and cyantraniliprole to L-02 cells was evaluated using the Cell Counting Kit-8 (CCK-8; BioScience Co. Ltd., Shanghai, China), according to the manufacturer's instructions. The cells were seeded into 96-well plates at a density of 1.2×10^4 cells/mL and exposed to varying concentrations of emamectin benzoate (0, 1, 3, 3.5, 4, and 4.5 μmol/L) and cyantraniliprole (0, 15, 30, 45, 60, 75, 100 μmol/L) in combination. Control cells were subjected to 0.1% DMSO alone. After 48 h of incubation, the absorbance at 450 nm was measured for each well using a SpectraMax M5 microplate reader (Molecular Devices, Sunnyvale,

CA, USA). Cell viability was calculated as a percentage compared with the corresponding solvent control. Each treatment was replicated six times.

Oxidative stress parameters response assays

The combined effect of pesticide exposure on oxidative stress in L-02 cells was assessed by measuring the activities of superoxide dismutase (SOD) and catalase (CAT), as well as the levels of reactive oxygen species (ROS), malondialdehyde (MDA), and glutathione (GSH). Briefly, the resuspended L-02 cells were seeded into six-well plates (1.6×10^5 cells/mL) and cultivated for 24 h. Subsequently, the cells were treated with emamectin benzoate (1, 3, 3.5, 4, and 4.5 μmol/L) and cyantraniliprole (15, 30, 45, 60, and 75 μmol/L) alone or their binary mixtures (3 + 15, 1 + 45, 4 + 15, and 4 + 45 μmol/L), and incubated for an additional 48 h. After treatment, the intracellular ROS levels were quantified using a dichlorofluorescein diacetate (DCFDA) probe assay. Moreover, the activities and levels of SOD, CAT, GSH, and MDA were determined using assay kits (Beyotime Biotechnology, Shanghai, China) following the manufacturer's protocol.

Combined action of mixture toxicity analysis

The combined toxicity of the mixture was evaluated by comparing the "measured values," which represented the examined endpoints, with the "theoretical values." These theoretical values were defined as the sum of toxic effect values induced by each chemical in isolation during individual exposure experiments. These theoretical values were calculated using the method outlined by Li et al.[21]. The significance of the difference between the measured and theoretical values was evaluated using a one-way analysis of variance (ANOVA) to determine the presence of any interactions. The interpretation of the results was as follows: (I) An additive effect was noted when the measured values did not significantly differ from the expected values. (II) A synergistic effect was identified when the measured values were significantly higher than the expected values. (III) An antagonistic effect was identified when the measured values were significantly lower than the expected values.

Untargeted metabolomic analysis

For the untargeted metabolomic analysis, four groups of L-02 cells were prepared: the control group consisted of normal cells treated with 0.1% DMSO, while the treatment groups were exposed to inhibitory concentrations at 10% of emamectin benzoate (4 μmol/L) and cyantraniliprole (45 μmol/L), as well as their respective mixtures. After cell culture and treatment, six biological replicate cell samples (with a density of 1×10^7 cells/mL) were collected using trypsin digestion and subsequent centrifugation. The intracellular metabolites were then extracted from the cell precipitates using the cold methanol extraction method. Briefly, the samples were resuspended in 1.0 mL of prechilled methanol–water solution (4:1, *v/v*), supplemented with 200 μL of chloroform. After breaking the cells for 3 min, 20 μL of isotope-labeled internal standard L-2-chlorophenylalanine (0.1 mg/mL) was added, and the mixture was subjected to ultrasonication for 20 min in an ice-water bath. After centrifugation at 13,000 rpm for 10 min, 800 μL of the supernatant was evaporated to dryness and redissolved in 300 μL of methanol–water solution (4:1, *v/v*) for metabolomic analysis.

The untargeted metabolomic analysis was performed using an ultra-performance liquid chromatography-quadrupole time-of-flight mass spectrometry (UPLC-Q-TOF/MS) system. Chromatographic separations were performed on a Waters ACQUITY UPLC I-Class system equipped with an HSS T3 C18 column (100 mm × 2.1 mm, 1.8 μm). The column oven temperature was maintained at 40 °C, and the injection volume was 5 μL. Mobile phases A (water containing 0.1% formic acid) and B (acetonitrile) were used in a gradient elution program at a flow rate of 0.35 mL/min: 0 min, 5% B; 2 min, 5% B; 4 min, 30% B; 8 min, 50% B; 10 min, 20% B; 14 min, 100% B; 15 min, 100% B; 15.1 min, 5% B; and 16 min, 5% B. Compound identification was performed using a Waters VION IMS QTOF mass spectrometer. The analytes were quantified using full scan MS under positive and negative modes with a mass range of *m/z* 100–1200. The resolution was set at 70,000 for full MS scans and 17,500 for HCD MS/MS scans. The optimal MS operating conditions were as follows: spray voltage of 3800 V (+) and 3000 V (−); sheath gas flow rate of 35 arb; auxiliary gas flow rate of 8 arb; and capillary temperature of 320 °C.

The quality control (QC) samples were injected after every six test samples to ensure the reproducibility of the analytical process. The QC samples exhibited distinct separation, and the replicated samples were closely clustered, confirming the consistency and reliability of the data (Supplementary Fig. S1). Metabolite profiling data underwent log2 transformation for subsequent statistical analysis and were normalized using Progenesis QI v 3.0 software (Nonlinear Dynamics, Newcastle, UK). The identification of differential metabolites was conducted using the Human Metabolome Database, LIPID MAPS (v2.3), METLIN database, and a self-built database (Lumingbio Co. Ltd., Shanghai, China). Visual representation of metabolic alterations among experimental groups was achieved using principal component analysis (PCA) and (orthogonal) partial least-squares-discriminant analysis (O)PLS-DA. Metabolites with VIP values of > 1.0, p-values < 0.05, and a fold change > 1.0 (for upregulated metabolites) or < 1.0 (for downregulated metabolites) were considered differential metabolites. The identified differential metabolites were then annotated using the Kyoto Encyclopedia of Genes and Genomes (KEGG) database (https://www.kegg.jp/) and subsequently mapped to the relevant pathways in which they are implicated.

Measurement of mitochondrial NADH/NAD$^+$ and ATP content assay

The NADH/NAD$^+$ and adenosine triphosphate (ATP) contents were measured using an assay kit (Nanjing Jiancheng Bioengineering Institute, Nanjing, China). The cells were seeded into 96-well plates at a density of 1.2×10^4 cells/mL and exposed to emamectin benzoate (4 μmol/L), cyantraniliprole (45 μmol/L), and their respective mixtures for 48 h. For NADH and NAD$^+$ cycling mix preparation, the manufacturer's protocol was followed, and measurements were conducted at 570 nm using a spectrophotometer (UV-2700i, SHIMADZU,

Shanghai, China). The NADH/NAD^+ redox ratio was computed based on the specific values of NADH and NAD^+ concentrations. The ATP level was determined according to the manufacturer's instructions and quantified at 636 nm.

Transmission electron microscopy (TEM) of mitochondria

The cells treated with emamectin benzoate (4 μM), cyantraniliprole (45 μM), and their respective mixtures were examined under a JEM-1200 TEM (JEOL Ltd., Tokyo, Japan). The samples were fixed in 2.5% glutaraldehyde for 24 h. After fixation, the samples were washed, dehydrated, and embedded in pure resin, according to the protocol of Zhao et al.[22]. Afterward, ultrathin sections (70–90 nm) obtained from the resin-embedded blocks using an ultramicrotome (EM UC7, Leica, Wetzlar, Germany) were observed and photographed.

Calculation of the BMD

A web-based system for Bayesian BMD estimation (https://benchmarkdose.com/) was used to calculate the BMD and its lower 95% confidence limit (BMDL), with a 5% benchmark response level[23]. In this approach, pesticide exposure dose was considered the dose parameter, and the contents of ROS were considered the response variable. The best-fitting model was determined according to the goodness of fit test $p > 0.05$ and maximum model weight.

Statistical analysis

The experiments were independently repeated at least three times, and the results are presented as the mean ± standard deviation (SD). R (version 4.2; R Development Core Team) was employed for data analysis and graphical representation. Significant differences between two groups were determined using a two-tailed unpaired t-test, while differences among multiple groups were evaluated using ANOVA.

Results and discussion

Toxic effect of pesticide mixture exposure on the liver

The serum biochemical parameters related to liver function, including ALT, AST, TBIL, DBIL, ALB, ALP, γ-GT, and TBA, were measured to elucidate the effect of exposure to the tested pesticide mixture on rat liver. The results indicated that the serum levels of ALT, AST, TBIL, and DBIL increased in the treatment groups of emamectin benzoate and cyantraniliprole compared with the control group (Supplementary Table S1). In contrast, exposure to the binary mixture of emamectin benzoate and cyantraniliprole resulted in synergistic toxic effects on liver function, with TBIL and DBIL levels increasing by more than 2.26-fold and 1.77-fold, respectively. These findings highlight the potential elevation of health risk due to residue mixtures of emamectin benzoate and cyantraniliprole.

Combined toxicity of pesticide residue mixtures to L-02 cells viability

The cell viability assessments demonstrated that exposure of L-02 cells to emamectin benzoate and cyantraniliprole individually for 48 h led to concentration-dependent decreases in viability (Fig. 1a,b). The corresponding 50% maximal effect (EC_{50}) values were determined as 6.21 μmol/L and 217.4 μmol/L, respectively. Exposures to their binary mixtures caused significantly lower cell viability than the individual exposures, with the frequency of synergism becoming more pronounced at higher exposures (Fig. 1c). Moreover, as the concentration ratio of emamectin benzoate in the mixture increased, a more pronounced reduction in cell viability was observed. For instance, co-treatment with 4 μmol/L, 4.5 μmol/L, and 5 μmol/L of emamectin benzoate combined with 15 μmol/L of cyantraniliprole yielded cell viabilities of 85.56%, 63.59%, and 43.21%, respectively. The approximate EC_{50} values for the inhibition of L-02 cells proliferation were determined in the combined exposures of 3 + 75 μmol/L, 3.5 + 75 μmol/L, 4 + 45 μmol/L, and 4.5 + 30 μmol/L.

Pesticides-induced oxidative stress in L-02 cells

Excessive oxidative stress can induce cellular damage and hinder proliferation, and oxidative events linked to cellular damage are recognized as major mechanisms underlying the toxic effects of environmental contaminants[24]. To evaluate whether the observed synergistic cytotoxicity was potentially caused by oxidative stress, intracellular ROS levels and MDA content were measured (Fig. 2a). In this study, exposure to emamectin benzoate (at concentrations ranging from 1 to 4.5 μmol/L) and cyantraniliprole (from 15 to 75 μmol/L) separately resulted in a dose-dependent increase in ROS levels (Supplementary Fig. S2). At higher pesticide concentrations, ROS production increased by 1.09-fold and 1.22-fold in cells exposed to emamectin benzoate and cyantraniliprole, respectively, compared with the control. Upon combined exposure, larger quantities of ROS were generated than those from single exposures. ANOVA of the combined toxicity mode unveiled that all the measured values significantly exceeded the theoretical values, indicating a synergistic effect (Fig. 2b). Among the combinations, the 3 + 15 μmol/L pesticide mixture exhibited the most pronounced synergistic effect, demonstrating the greatest discrepancy between the theoretical and measured values. Elevated ROS levels are a pivotal indicator of oxidative stress occurrence, often leading to redox imbalance and oxidative damage[25]. The results suggested that L-02 cells exposed to the binary mixture suffered increased oxidative damage compared with those exposed to these pesticides individually. Moreover, most combination-treated doses demonstrated a synergistic interaction in terms of MDA content, a parameter indicative of oxidative damage (Fig. 2c). This can be attributed to excessive ROS production and increased susceptibility to lipid peroxidation. Similar increases in ROS, leading to a substantial increase in MDA, have been observed using other pesticides, such as dimethoate[26] and triticonazole[27] separately.

Simultaneously, it is important to note that the generation of ROS and MDA can be counteracted by antioxidant defense systems. Thus, the activities of key antioxidant enzymes (SOD and CAT), along with GSH

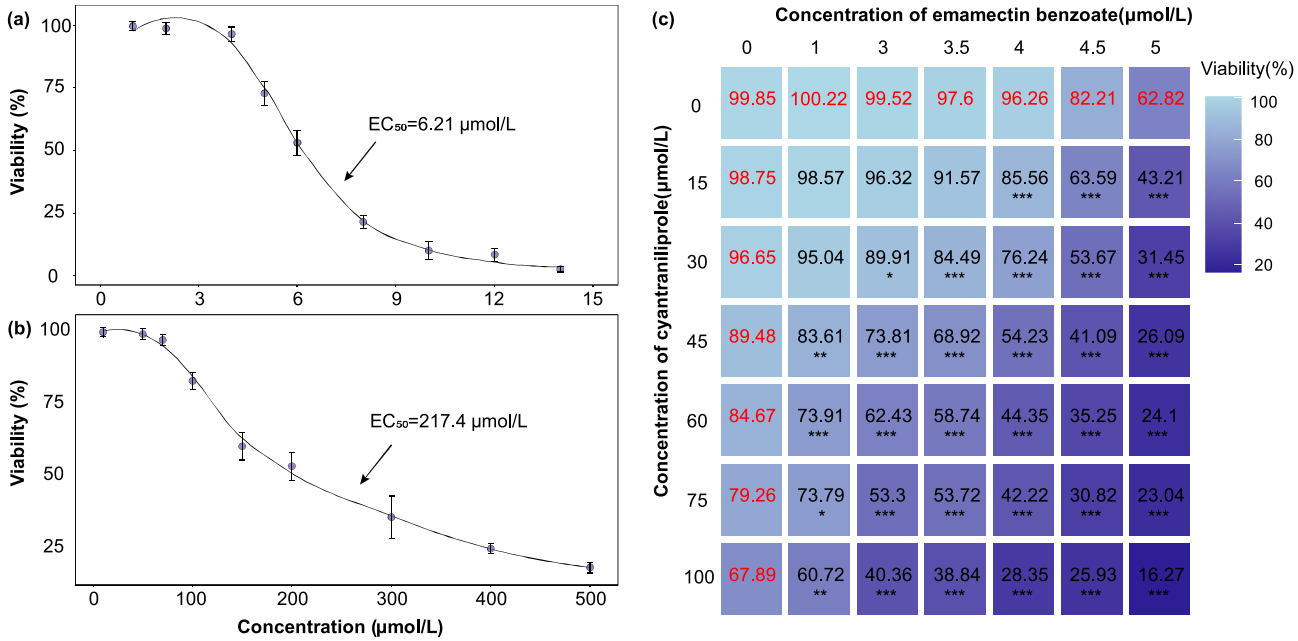

Fig. 1. Cell viability of L-02 cells exposed to (**a**) emamectin benzoate, (**b**) cyantraniliprole and (**c**) their combinations at different concentration ratios for 48 h. Results are presented as means ± SD of six independent experiments. $^{*}p < 0.05$, $^{**}p < 0.01$, and $^{***}p < 0.001$ indicate statistical differences from control of a single pesticide by one-way ANOVA, respectively. The red font represents the exposure of L-02 cells to emamectin benzoate or cyantraniliprole individually for 48 h in viability assays.

levels, were assessed to better understand the mechanism underlying oxidative damage. Emamectin benzoate and cyantraniliprole exposures increased SOD and CAT activities, as well as GSH contents (Fig. S2). The measured values for binary mixtures were significantly higher than the theoretical values, except SOD and CAT in the 3 + 15 μmol/L combination and CAT in the 4 + 45 μmol/L combination (Fig. 2d–f). This observation signifies the presence of either an additive or synergistic effect. This increase in antioxidant enzyme activity may be attributed to the prevention of excessive ROS and/or MDA production. However, in instances where oxidative damage is particularly severe, surpassing the cell's inherent repair capacity, cellular damage, and even apoptosis can ensue. Therefore, the synergistic cytotoxicity that impairs L-02 cells proliferation is likely driven by excessive oxidative stress.

Identification of metabolic profiles in response to pesticide mixtures

To identify potential biomarkers for monitoring the combined toxicity of pesticide mixtures, an untargeted metabolomic analysis was conducted. This approach involved comparing the metabolic profiles among cells treated with different conditions: solvent control (DMSO), individual pesticides, and their combination. The analysis revealed a comprehensive spectrum of 3,969 detected metabolites, which were classified into nine recognized classes. These included benzene and substituted derivatives (n = 241), carboxylic acids and derivatives (n = 639), fatty acyls (n = 475), glycerophospholipids (n = 199), organooxygen compounds (n = 319), polyketides (n = 82), prenol lipids (n = 136), steroids and steroid derivatives (n = 106), and other metabolites (n = 1772) (Supplementary Fig. S3). Detailed information on all the identified metabolites is shown in Table S2. To comprehensively assess the differences in metabolite profiles among the various treatment groups, multivariate statistical analyses were performed (Fig. 3). The PCA score plot distinctly separated the metabolite profiles among the four treatment groups, with the first principal component (PC1) and second principal component (PC2) accounting for 45.0% of the total variance (Fig. 3a). The PCA plots revealed significant metabolic differences between the three treatment groups and the control group. To maximize the sample group separation and identify different biomarkers, pairwise comparisons were achieved using the PLS-DA and OPLS-DA models. In the (O)PLS-DA score plots and corresponding S-plots, the four treatment groups were also well separated in pairs. High predictability ($Q^2 \geq 0.93$) and strong goodness of fit ($R^2X \geq 0.64$, $R^2Y \geq 0.99$) were observed in the pairwise comparison. Additionally, 200 iterations of response permutation tests confirmed that the OPLS-DA models were not overfitted.

The molecules with a VIP of > 1.0, as analyzed using the OPLS-DA models, were used to generate the volcano plot. As shown in Fig. 4a, metabolites with p-values < 0.05 were considered significant and were used to identify potential markers of synergistic toxicity. Using these criteria, we identified 251 significant differential metabolites (149 upregulated and 102 downregulated) in the comparison group of emamectin benzoate (EB vs. CK), 317 significant differential metabolites (164 upregulated and 153 downregulated) in the comparison group of cyantraniliprole (CA vs. CK), and 268 significant differential metabolites (167 upregulated and 101 downregulated) in the combination group (EBCA vs. CK) with the control. Furthermore, we observed 284

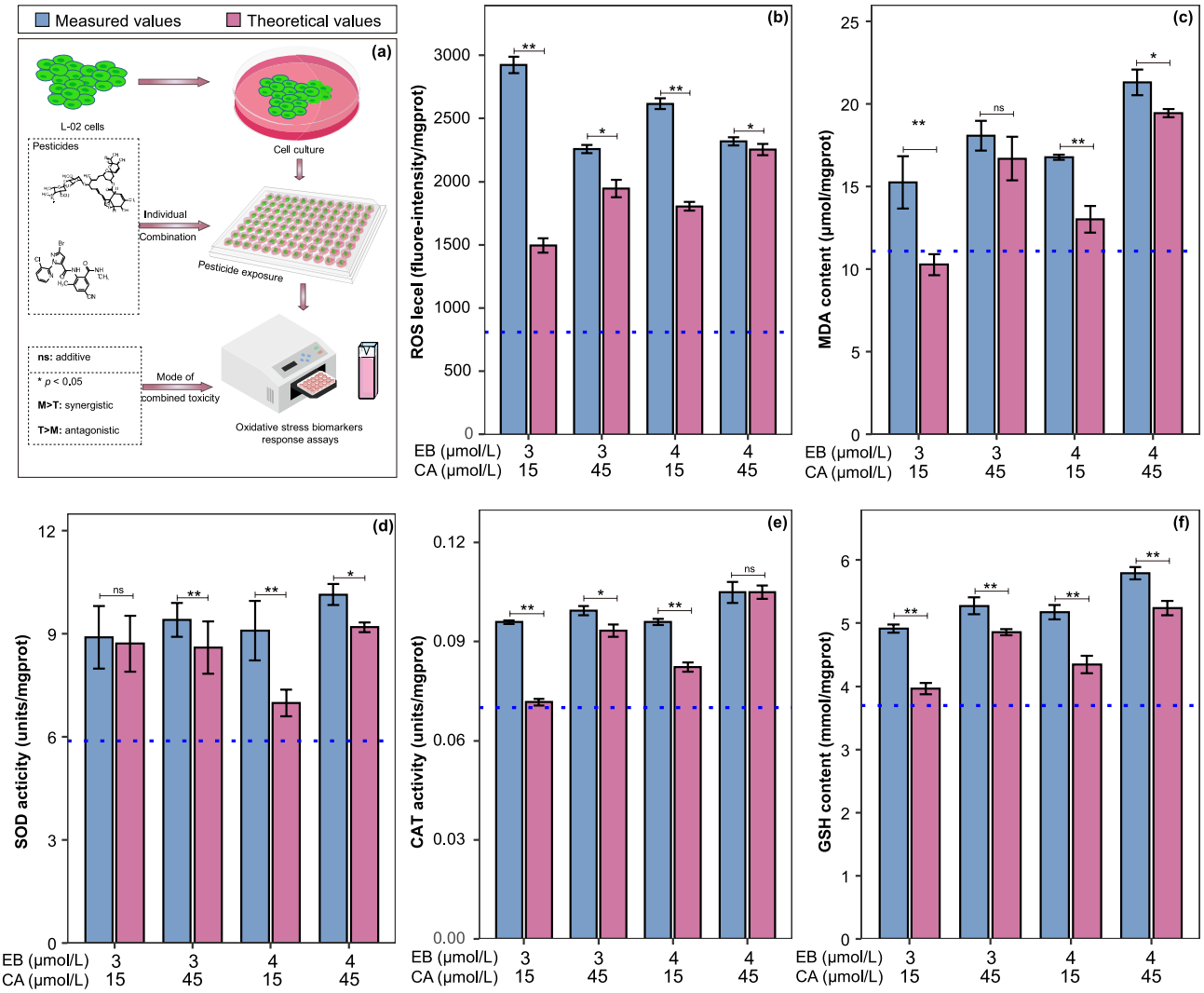

Fig. 2. Oxidative stress response to binary mixture-induced toxicity and the combined action of emamectin benzoate and cyantraniliprole at combination of 3 + 15 μmol/L, 3 + 45 μmol/L, 4 + 15 μmol/L, and 4 + 45 μmol/L. (**a**) Schematic overview of oxidative stress biomarkers assays and combined action analysis. Activity and content of intracellular (**b**) ROS, (**c**) MDA, (**d**) SOD, (**e**) CAT, and (**f**) GSH after exposure to binary mixture. $^{*}p < 0.05$ and $^{**}p < 0.01$ indicate difference between the theorical values and measured values, respectively, which represents synergistic effect when the measured values were significantly higher than the expected values. ns showed no significant difference in statistics and was recorded as a additive effect. The combined action was evaluated by comparing the "measured values (M)", which corresponded to the examined endpoints, against the "theoretical values (T)".

metabolites that significantly differed in the comparison group of the pesticide mixtures and emamectin benzoate (EB vs. EBCA), as well as 188 in the comparison group of the pesticide mixtures and cyantraniliprole (CA vs. EBCA). Subsequently, a Venn diagram was used to visualize and filter the overlapping and specific differential metabolites among the treatment groups (Fig. 4b). By comparing the groups of EB vs. CK and CA vs. CK, 44 metabolites were specifically altered in EBCA vs. CK, of which most were upregulated (n = 30), with the majority being the superclasses of lipids and lipid-like molecules (e.g., glycerophospholipids and fatty acyls), organic acids and derivatives, and organic oxygen compounds (Supplementary Table S3). Among the overlapping differential metabolites (n = 104) in the three pairwise comparisons, 67 were associated with oxidative stress; they were mostly in the classes of glycerophospholipids, fatty acyls, and carboxylic acids and derivatives (Supplementary Table S4). Similarly, 76.12% of the overlapping differential metabolites in the pairwise comparisons of EB vs. EBCA and CA vs. EBCA also belonged to these three categories (Supplementary Table S5). Previous studies have demonstrated that the glycerophospholipid metabolism pathway plays a crucial role in oxidative stress[28]. Substantial alterations in fatty acyl profiles can cause the accumulation of lipid peroxidation products, which are susceptible to mitochondrial oxidative damage[29]. The pattern of highly organooxygen compound profiles is associated with oxidative stress[30]. Consequently, these metabolites might be potential biomarkers for predicting manifestations of oxidative stress.

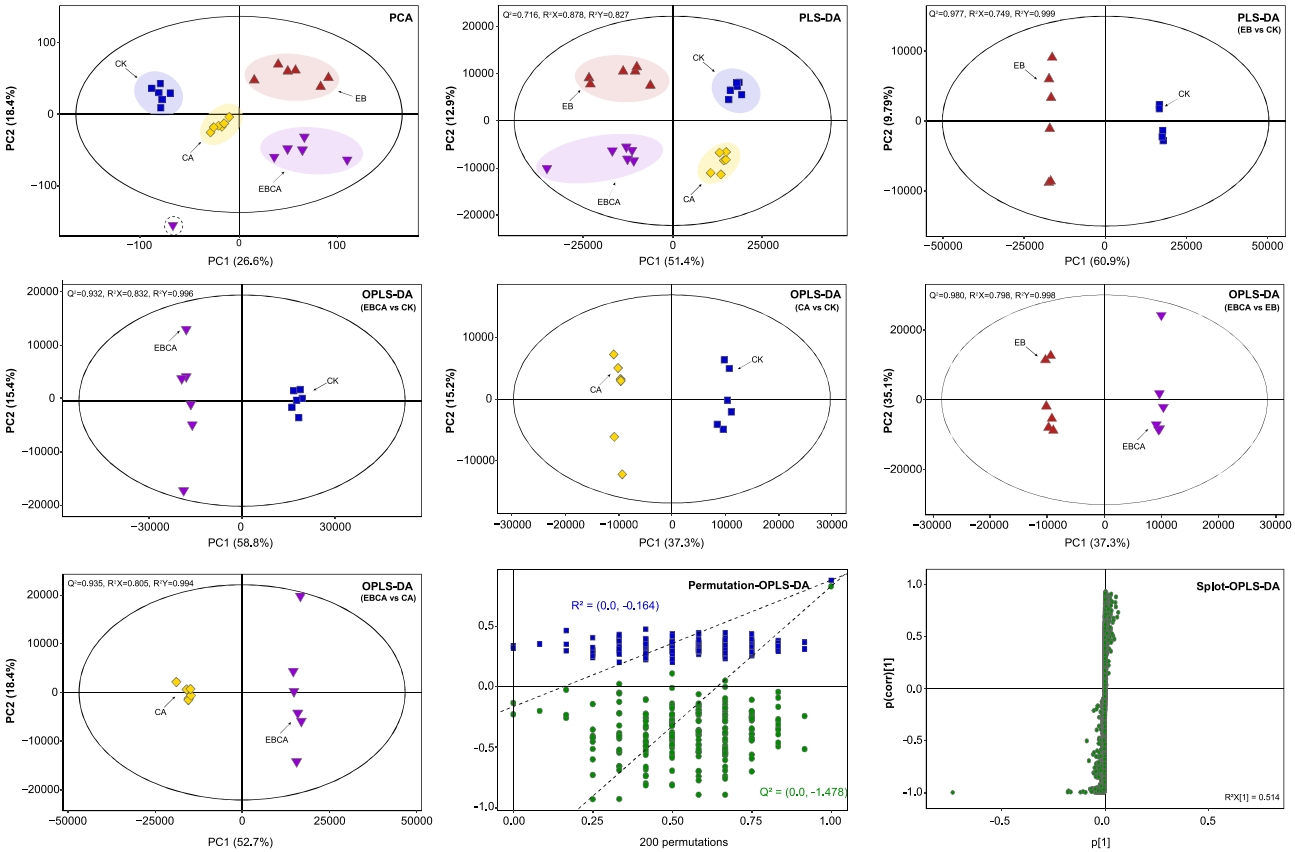

Fig. 3. Multivariate statistical analyses of metabolites in the pairwise comparisons of solvent control (DMSO), individual pesticides and their combination. CK, EB, CA, and EBCA represents solvent control, emamectin benzoate, cyantraniliprole, and their binary mixture, respectively.

KEGG classification and enrichment analysis of differential metabolites

The metabolic pathway analysis for the identification of significant differential metabolites was further classified according to the KEGG annotation. In the comparison groups of EB vs. CK, CA vs. CK, and EBCA vs. CK, seven of the top 20 KEGG clusters were found to be commonly annotated and were primarily associated with oxidative stress processes. They included D-Amino acid metabolism, pantothenate and CoA biosynthesis, choline metabolism in cancer, ABC transporters, neuroactive ligand-receptor interaction, pyrimidine metabolism, and beta-alanine metabolism. The outcomes indicated a similar or common mechanism of toxic effects of emamectin benzoate and cyantraniliprole on oxidative stress in L-02 cells (Fig. S4a). Groups EB vs. EBCA and CA vs. EBCA can also be observed for many metabolites that map to the mitochondrial oxidative stress-related metabolic pathways, such as ABC transporters, pantothenate and CoA biosynthesis, and aminoacyl-tRNA biosynthesis (Fig. S4b). Mitochondria play an important role in energy metabolism, control of stress responses, and biosynthetic processes[31]. Barrera et al. reported that the imbalance in the mitochondrial dynamic process causes increased lipid peroxidation, high ROS generation, decreased membrane potential, and reduced ATP synthesis[26]. Moreover, mitochondria are a major source of cellular ROS production, which in turn is a primary target of ROS attacks. Therefore, the possible metabolic mechanism underlying synergistic cytotoxicity may be the aggravated production of ROS, which greatly exceeds the antioxidant protection of L-02 cells, leading to an imbalance in mitochondrial oxidation and energy metabolism (Fig. 5a).

Mitochondrial dysfunction analysis

To further verify our findings, three indicators (NADH/NAD$^+$ redox ratio, ATP, and mitochondrial morphology) associated with mitochondrial dysfunction were analyzed. The NADH/NAD$^+$ redox index is crucial in regulating the intracellular redox state and is tightly linked to the tricarboxylic acid cycle (TCA cycle). This study indicated that the NADH/NAD$^+$ ratio was significantly elevated in the treatment groups compared with the solvent control (Fig. 5b). An increase in mitochondrial NADH content suggests enhanced cellular oxygen consumption and inhibition of the TCA cycle, leading to concomitant ROS generation[32]. Synergistic effects were observed in the binary pesticide combination (4 + 45 μmol/L), increasing the NADH/NAD$^+$ ratio by more than three times. This observation demonstrated that the possible metabolic mechanism underlying synergistic cytotoxicity may be the aggravated production of ROS. Generally, complex I oxidizes NADH to NAD$^+$, generating electron flow to ubiquinone to drive ATP synthesis[33]. Consequently, an increase in NADH content may induce a decrease in ATP content. This study demonstrated that exposure to the pesticide mixture resulted in a significant reduction

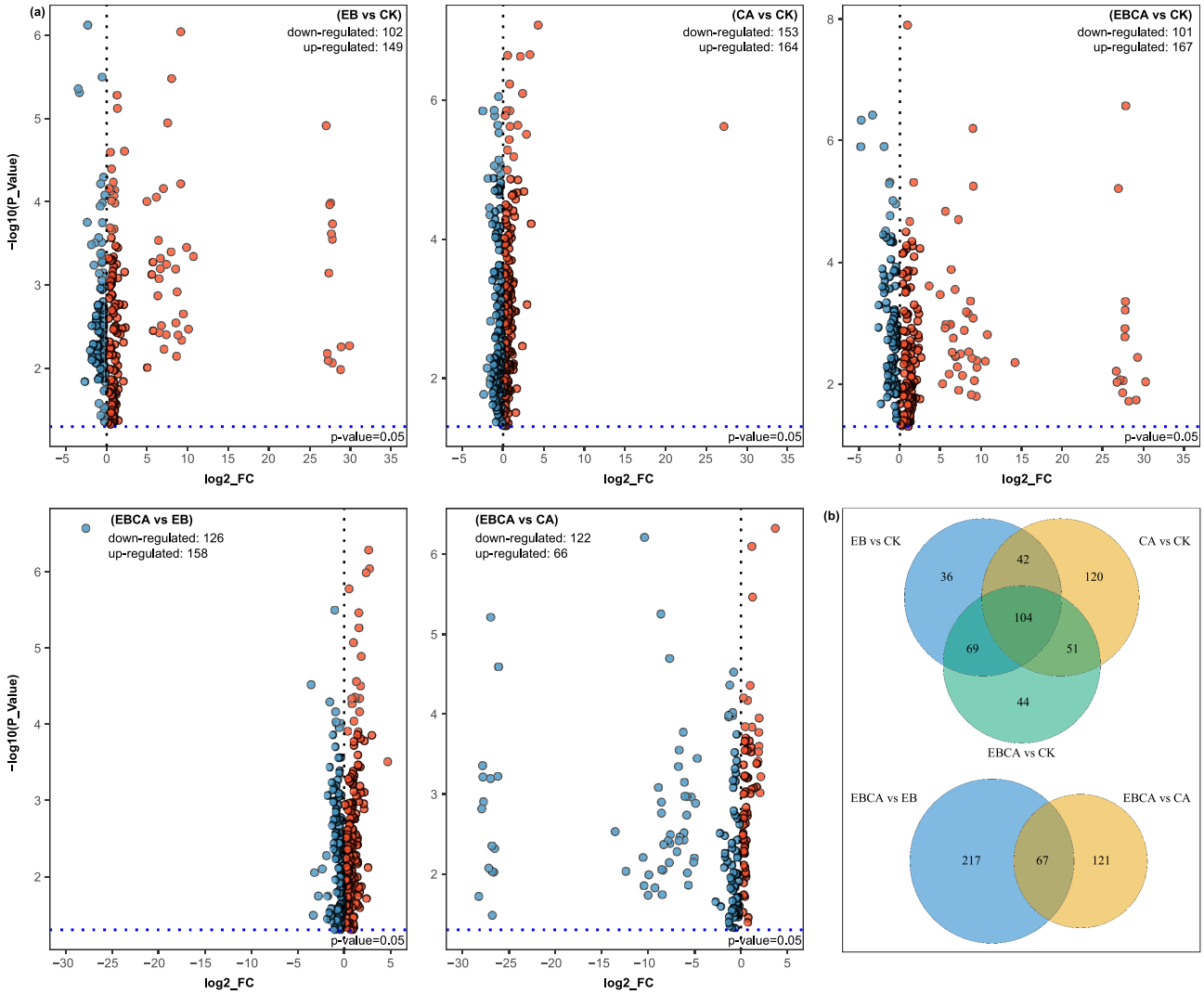

Fig. 4. (**a**) Volcano plot and (**b**) venn diagram analyses for significantly different metabolites in the pairwise comparisons emamectin benzoate (EB vs CK), cyantraniliprole (CA vs CK), and their combination (EBCA vs CK) with controls, respectively.

in ATP content by 34.77% compared with the control (Fig. 5c). ATP serves as a vital intracellular energy source produced in mitochondria, and its depletion indicates an imbalance in energy metabolism[34]. Representative TEM micrographs further confirmed mitochondrial dysfunction in L-02 cells exposed to the treatment groups (Fig. 5d). Briefly, compared with the control group, a conspicuous increase in the percentage of autophagy and swelling was observed in L-02 cells treated with individual pesticides. The swollen mitochondria displayed expanded matrix space and fragmented or disorganized cristae. The extent of mitochondrial morphological damage was pronounced with their combined exposure. In summary, the synergistic cytotoxicity of the binary pesticide combination to L-02 cells is likely driven by aggravated production of ROS.

Combined toxicity threshold based on BMD analysis

Based on the above findings, ROS was identified as the key endpoint to monitor the combined toxicity of emamectin benzoate and cyantraniliprole. The BMD model is considered a better approach than the NOAEL in deriving toxicity thresholds[35]. Therefore, a quantitative analysis of the dose–response relationship between the endpoint and concentration of pesticides using BMD calculations was performed. Supplementary Table S6 summarizes the results of the different models automatically calculated according to the default conditions. The model-averaged estimates of the BMDLs of the binary mixtures at concentration ratios of 3:15, 3:45, 4:15, and 4:45 were 4.74 mmol/L, 9.58 mmol/L, 6.01 mmol/L, and 7.52 mmol/L, respectively. The obtained BMDL values of the binary mixtures were 20% more toxic than their individual active ingredients (emamectin benzoate, 0.92 mM; cyantraniliprole, 11.68 mM) within the mixture except for the concentration ratio of 4:15. These findings highlight the need to consider synergistic toxicity in pesticide residue risk assessments.

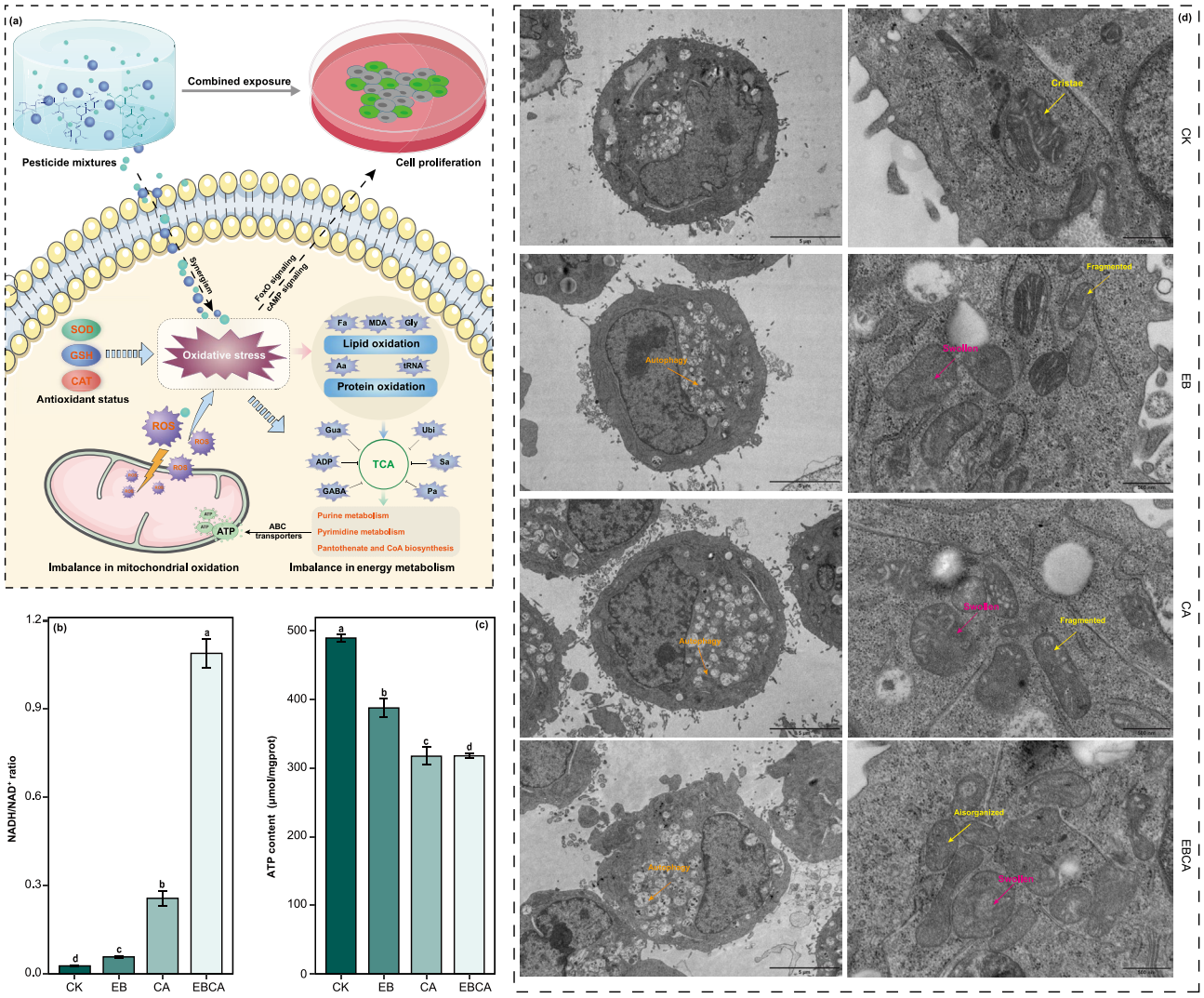

Fig. 5. (**a**) Schematic illustration for the possible metabolic mechanism of binary mixture-induced oxidative stress and synergistic toxicity in L-02 cells. (**b**) NADH/NAD$^+$ redox ratios, (**c**) ATP, and (**d**) mitochondrial morphology of L-02 cells exposed to control, emamectin benzoate (EB; 4 μmol/L), cyantraniliprole (CA; 45 μmol/L), and their combination (EBCA; 4 + 45 μmol/L) were analyzed, respectively. Fa (fatty acyls), Gly (glycerophosphoethanolamines), Aa (amino acids, including glutamine, pyroglutamic acid, N-acetylaspartylglutamic acid), tRNA (aminoacyl-tRNA), Gua (guanosine), ADP (adenosine diphosphate), GABA (γ-aminobutyric acid), Ubi (ubiquinone), Sa (succinic acid), Pa (pantothenic acid), TCA (tricarboxylic acid cycle), ATP (adenosine triphosphate) represent potential metabolites and/or pathways involved in the oxidative stress response. Bars with different lowercase letters are significantly different ($p < 0.05$). Ultra-structure (Scale bar = 5 μm & 500 mm) of the mitochondria from the control, as well as EB, CA, and EBCA-exposed groups.

Conclusions

Herein, we estimated the combined toxicity and interactions of emamectin benzoate and cyantraniliprole on L-02 cells. The results revealed that the binary mixtures produced either an additive or synergistic effect in increasing cell proliferation inhibition and excessive oxidative stress. We also observed a remarkable increase in serum biochemical parameters (TBIL and DBIL) related to rat liver function when rat liver, suggesting a potential elevation of health risk when exposed to the binary mixtures. The synergistic cytotoxicity observed in L-02 cells exposed to the pesticide mixture is primarily mediated by the induction of oxidative stress, highlighting ROS as a possible effective toxicity endpoint for predicting the combined toxicity threshold. Further research and investigations are required to in vivo studies to validate our results and assess their relevance to human health.

Data availability

Data is provided within the manuscript or supplementary information files.

Received: 8 January 2025; Accepted: 13 May 2025
Published online: 16 May 2025

References

1. Cui, K. et al. Health risks to dietary neonicotinoids are low for Chinese residents based on an analysis of 13 daily-consumed foods. *Environ. Int.* **149**, 106385 (2021).
2. Ma, J. M. et al. Rapid screening of 420 pesticide residues in fruits and vegetables using ultra high performance liquid chromatography combined with quadrupole-time of flight mass spectrometry. *Food Sci Hum. Well.* **12**, 1064–1070 (2023).
3. Martin, O. et al. Ten years of research on synergisms and antagonisms in chemical mixtures: A systematic review and quantitative reappraisal of mixture studies. *Environ. Int.* **146**, 106206 (2021).
4. Arlos, M. J., Focks, A., Hollender, J. & Stamm, C. Improving risk assessment by predicting the survival of field gammarids exposed to dynamic pesticide mixtures. *Environ. Environ. Sci. Technol.* **54**(19), 12383–12392 (2020).
5. Huang, P., Liu, S. S., Xu, Y. Q., Wang, Y. & Wang, Z. J. Combined lethal toxicities of pesticides with similar structures to *Caenorhabditis elegans* are not necessarily concentration additives. *Environ. Pollut.* **286**, 117207 (2021).
6. Liu, H. L. et al. Exposure to copper oxide nanoparticles triggers oxidative stress and endoplasmic reticulum (ER)-stress induced toxicology and apoptosis in male rat liver and BRL-3A cell. *J. Hazard. Mater.* **401**, 123349 (2021).
7. Te, J. A., AbdulHameed, D. M. & Wallqvist, A. Systems toxicology of chemically induced liver and kidney injuries: Histopathology-associated gene co-expression modules. *J. Appl. Toxicol.* **36**(9), 1137–1149 (2016).
8. Annoscia, D. et al. Neonicotinoid Clothianidin reduces honey bee immune response and contributes to Varroa mite proliferation. *Nat. Commun.* **11**(1), 5887 (2020).
9. Tosi, S., Sfeir, C., Carnesecchi, E., vanEngelsdorp, D. & Chauzat, M. P. Lethal, sublethal, and combined effects of pesticides on bees: A meta-analysis and new risk assessment tools. *Sci. Total. Environ.* **844**, 156857 (2022).
10. Ma, L. L. et al. Metabolomics and mass spectrometry imaging reveal the chronic toxicity of indoxacarb to adult zebrafish (*Danio rerio*) livers. *J. Hazard. Mater.* **453**, 131304 (2023).
11. Wang, R. F. et al. Residue and dissipation of two formulations of emamectin benzoate in tender cowpea and old cowpea and a risk assessment of dietary intake. *Food Chem.* **361**, 130043 (2021).
12. Wang, W. G. et al. The health risk of acetochlor metabolite CMEPA is associated with lipid accumulation induced liver injury. *Environ. Pollut.* **331**, 121857 (2023).
13. VoPham, T. et al. Pesticide exposure and hepatocellular carcinoma risk: A case-control study using a geographic information system (GIS) to link SEER-Medicare and California pesticide data. *Environ. Res.* **143**, 68–82 (2015).
14. Crouchet, E. et al. A human liver cell-based system modeling a clinical prognostic liver signature for therapeutic discovery. *Nat. Commun.* **12**(1), 5525 (2021).
15. Zhang, R. J. et al. Metabolomics analysis of the 3D L-02 cell cultures revealing the key role of metabolism of amino acids in ameliorating hepatotoxicity of perfluorooctanoic acid. *Sci. Total. Environ.* **806**, 150438 (2022).
16. Zhang, R. J., Yao, Y., Tu, L. Y., Luan, T. G. & Chen, B. W. Non-targeted metabolomics of multiple human cells revealing differential toxic effects of perfluorooctanoic acid. *J. Hazard. Mater.* **409**, 125017 (2021).
17. Ouyang, X., Fang, Q., Chen, A. & Huang, J. Effects of trunk injection with emamectin benzoate on arthropod diversity. *Pest Manag. Sci.* **79**(3), 935–946 (2023).
18. Cao, D. et al. Uptake, translocation, and distribution of cyantraniliprole in a wheat planting system. *J. Agric. Food Chem.* **71**(13), 5127–5135 (2023).
19. Moustafa, M. A. M. et al. In vitro and silico exploration of the insecticidal properties of *Lavandula multifida* L. essential oil and its binary combinations with cyantraniliprole and emamectin benzoate on *Spodoptera frugiperda* (Lepidoptera: Noctuidae). *Crop Prot.* **187**, 106969 (2024).
20. Yun, X. M. et al. A comparative assessment of cytotoxicity of commonly used agricultural insecticides to human and insect cells. *Ecotoxicol. Environ. Safe.* **137**, 179–185 (2017).
21. Li, X. H., Yin, P. H. & Zhao, L. Effects of individual and combined toxicity of bisphenol A, dibutyl phthalate and cadmium on oxidative stress and genotoxicity in HepG 2 cells. *Food Chem. Toxicol.* **105**, 73–81 (2017).
22. Zhao, D. et al. Complementary imaging of nanoclusters interacting with mitochondria via stimulated emission depletion and scanning transmission electron microscopy. *J. Hazard. Mater.* **465**, 133371 (2014).
23. Shao, K. & Shapiro, A. J. A web-based system for Bayesian benchmark dose estimation. *Environ. Health Persp.* **126**(01), 017002 (2018).
24. Zheng, F. L. et al. Redox toxicology of environmental chemicals causing oxidative stress. *Redox Biol.* **34**, 101475 (2020).
25. Shadfar, S., Parakh, S., Jamali, M. S. & Atkin, J. D. Redox dysregulation as a driver for DNA damage and its relationship to neurodegenerative diseases. *Transl. Neurodegener.* **12**(1), 18 (2023).
26. Barrera, G. et al. Mitochondrial dysfunction in cancer and neurodegenerative diseases: Spotlight on fatty acid oxidation and lipoperoxidation products. *Antioxidants* **5**(1), 7 (2016).
27. Liu, R. et al. Enantioselective mechanism of toxic effects of triticonazole against Chlorella pyrenoidosa. *Ecotox. Environ. Safe.* **185**, 109691 (2019).
28. Dang, V. T., Zhong, L. H., Huang, A., Deng, A. & Werstuck, G. H. Glycosphingolipids promote pro-atherogenic pathways in the pathogenesis of hyperglycemia-induced accelerated atherosclerosis. *Metabolomics* **14**, 92 (2018).
29. Malý, M. et al. Lipidomic analysis to assess oxidative stress in acute coronary syndrome and acute stroke patients. *Metabolites* **11**(7), 412 (2021).
30. Chen, C. S., Yuan, T. H., Shie, R. H., Wu, K. Y. & Chan, C. C. Linking sources to early effects by profiling urine metabolome of residents living near oil refineries and coal-fired power plants. *Environ. Int.* **102**, 87–96 (2017).
31. Hanada, Y. et al. MAVS is energized by Mff which senses mitochondrial metabolism via AMPK for acute antiviral immunity. *Nat. Commun.* **11**(1), 5711 (2020).
32. Tapias, V., McCoy, J. L. & Greenamyre, J. T. Phenothiazine normalizes the NADH/NAD(+) ratio, maintains mitochondrial integrity and protects the nigrostriatal dopamine system in a chronic rotenone model of Parkinson's disease. *Redox Biol.* **24**, 101164 (2019).
33. Liu, J. H. et al. Mitochondria-targeting single-layered graphene quantum dots with dual recognition sites for ATP imaging in living cells. *Nanoscale* **10**(36), 17402–17408 (2018).
34. Paggio, A. et al. Identification of an ATP-sensitive potassium channel in mitochondria. *Nature* **572**(7771), 609–613 (2019).
35. Haber, L. T. et al. Benchmark dose (BMD) modeling: Current practice, issues, and challenges. *Crit. Rev. Toxicol.* **48**, 387–415 (2018).

Author contributions

Y.X.Z., Y.X.X., and J.J.X. designed the study, Y.X.Z., Y.X.X., Z.Y.C., and K.J.D. performed the experiment, Y.Y.L. and Z.Q.L. analyzed the data, Y.H.S. and H.Q.C. commented on the manuscript, J.J.X. wrote the manuscript. All authors reviewed the manuscript.

Funding
This work was supported by the University Outstanding Youth Talent of Anhui Province (2023AH030048), National Natural Science Foundation of China (32102245), Natural Science Foundation of Anhui Province (2108085QC116), Research Funds of Joint Research Center for Food Nutrition and Health of IHM (2024SJY03), and Undergraduate Innovation and Entrepreneurship Training Program (S202210364253 and X202310364506).

Declarations

Ethics approval and consent to participate
All methods were performed in accordance with the relevant guidelines and regulations. The animal care and experimental protocols were approved by the Guidelines of the Institutional Animal Care Committee of Anhui Agricultural University (AHAUXMSQ 2024094).

Competing interests
The authors declare no competing interests.

Additional information
Supplementary Information The online version contains supplementary material available at https://doi.org/10.1038/s41598-025-02429-6.

Correspondence and requests for materials should be addressed to J.X.

Reprints and permissions information is available at www.nature.com/reprints.

Publisher's note Springer Nature remains neutral with regard to jurisdictional claims in published maps and institutional affiliations.